#6180

NUMERICAL SIMULATION OF 2-D AND 3-D NON-STEADY TURBULENT GAS MIXTURE FLOWS WITH LARGE DENSITY GRADIENTS IN VENTILATION SYSTEMS

I.N.Korolyova , D.A.Niculin and M.Kh.Strelets
State Institute for Applied Chemistry
St.-Petersburg, Russia

SUMMARY

A mathematical model for low Mach number turbulent mixed convection of a gas mixture is developed. The model is based on the asymptotic (zero Mach number) form of full Reynolds equations, which are closed with the "k-ε" turbulence model and so-called wall functions approach to account for the molecular-turbulent transfer interaction near the solid walls. An important advantage of the model, being proposed, over traditional Boussinesq approximation, is its applicability for the description of flows with high density gradients, caused by strong spatial non-uniformity of species concentration and/or temperature, which are quite typical for ventilation.

For the numerical integration of the governing equations of the model an appropriate modification of the well known semi-implicit SMAC-method is used. The capabilities of the proposed technique are illustrated by some examples of the simulation of 2-D and 3-D turbulent ventilation flows of air/contaminating gas mixtures in rooms with different geometries. A comparison of the predicted results with experimental data is also presented.

NUMERICAL SIMULATION OF 2-D AND 3-D NON-STEADY TURBULENT GAS MIXTURE FLOWS WITH LARGE DENSITY GRADIENTS IN VENTILATION SYSTEMS

I.N.Korolyova , D.A.Niculin and M.Kh.Strelets
State Institute for Applied Chemistry
St.-Petersburg, Russia

NOTATION

C Contaminating gas mass concentration

C_1, C_2, c_μ Constants of turbulence model

$D_{1,2}$ Binary diffusion coefficient

D_t Turbulent diffusion coefficient

E Log-law constant (=9.793)

$\hat{E}$ Unit tensor

Fr Froude number

G_k Generation of turbulence energy

$\vec{g}$ Gravitational vector (0,0,-g)

g Acceleration due to gravity(=9.8)

H Height of room

k Turbulent kinetic energy

n Normal direction

p Pressure

$\vec{r}$ Radius-vector

Re Reynolds number

$\hat{S}$ Deformation tensor

Sc Schmidt number

ε Dissipation rate of turbulent energy

ε_m Non-dimensional difference of molecular weight $(=(m_2 - m_1)/m_1)$

G averaged mass fraction

κ Von Karman constant (=0.41)

μ Viscosity

ρ Density

$\sigma_k, \sigma_\varepsilon$ Constant of turbulence model

$\hat{\tau}$ Shear stress tensor

τ Time step

Ω Volume of room

Subscripts

- $_{eff}$ Effective value
- $_{p}$ Value relating to mesh node "p"
- $_{t}$ Turbulent value
- $_{w}$ Wall value

Superscripts

- ^{n} Value at new time level
- ^{o} Value at old time level
- ^{k} Value at current iteration

INTRODUCTION

An overwhelming majority of the contemporary works dealing with the numerical simulation of forced and mixed convection in ventilation systems are based on the classical model of incompressible flow or so-called Boussinesq approximation, see e.g. Rheinlander [1] and Nielsen [2,3]. It's well known, however, that these models are valid only for a flow with a relatively weak density variation.

At the same time, for many situations important from the viewpoint of practical application, density variations may by strong enough because of a significant non-uniformity of the temperature and/or species concentrations distribution inside a ventilated room. For example, in air ventilation systems with natural gas contamination, even in an isothermal case, the density of the mixture may vary by a factor of 1.66, and with hydrogen contamination - by a factor of 15. It's quite clear that an incompressible flow model and the Boussinesq approximation are absolutely unusable for modeling of such ventilation processes. On the other hand, because of the acoustic stiffness of the full Navier-Stokes equations for slow flows (Mach number $M << 1$), the Navier-Stokes simulation of ventilation systems, whose generic feature is the low value of the flow Mach number, presents rather difficult computational problems.(see. e.g. Oran & Boris [4], Mcdonald [5], Lapin & Strelets [6].

To overcome these difficulties special complicated numerical algorithms,e.g. such as [7,8], are needed. So the optimal approach to the numerical simulation of ventilation flows seems to be the use of a so-called hyposonic flow model which is the asymptotic form of the full Navier-Stokes equations when $M \to 0$ [6].From the viewpoint of the full description of ventilation flows, this model is practically equivalent to the Navier-Stokes equations, but from the point of view of computational complexity it s almost the same as an incompressible flow model or Boussinesq approximation. Previously the authors have successfully used hyposonic flow model [6] for the numerical simulation of laminar flow in ventilating systems [9, 10]. In the present work this model is extended to turbulent regimes of such flows. A brief description of proposed model and corresponding finite-difference scheme

along with same results of computer code testing and examples of the application of this code to the numerical simulation of 2-D and 3-D unsteady ventilation turbulent flow are presented.

GOVERNING EQUATIONS AND NUMERICAL METHOD

The asymptotic (slow flow) conservation equations for the averaged turbulent flow quantities may be derived by the averaging of the corresponding equations of the hyposonic flow model, proposed by Lapin & Strelets [6], which represents the asymptotic form of the full Navier-Stokes system at the limit case of the flow Mach number and the hydrostatic compressibility parameter equal to zero. For the special case of a turbulent isothermal binary gas mixture flow, being considered in the present work, the governing equations of the model, derived in such a way, may be written in the following non-dimensional form:

$$\rho \frac{\partial \vec{V}}{\partial t} + (\rho \vec{V} \cdot \frac{\partial}{\partial \vec{r}}) \vec{V} = - \frac{\partial p}{\partial \vec{r}} + \frac{2}{Re} \frac{\partial}{\partial \vec{r}} \cdot (\hat{\tau}_{eff}) + \frac{1}{\varepsilon_* Fr} (\rho - 1) \frac{\vec{g}}{g}, \quad (1)$$

$$\rho \frac{\partial}{\partial \vec{r}} \cdot \vec{V} = \frac{1}{Re\, Sc} \frac{\varepsilon_*}{(C\varepsilon_* + 1)} \frac{\partial}{\partial \vec{r}} \cdot (D_{eff} \frac{\partial C}{\partial \vec{r}}), \quad (2)$$

$$\rho \frac{\partial C}{\partial t} + \rho \vec{V} \cdot \frac{\partial C}{\partial \vec{r}} = \frac{1}{Re\, Sc} \frac{\partial}{\partial \vec{r}} \cdot (D_{eff} \frac{\partial C}{\partial \vec{r}}), \quad (3)$$

$$\rho (C\varepsilon_* + 1) = 1. \quad (4)$$

As mentioned above, the system (1)-(4) is closed by the following modification of the"k-ε"turbulence model [11,12]:

$$\rho \frac{\partial k}{\partial t} + \rho \vec{V} \cdot \frac{\partial k}{\partial \vec{r}} = \frac{1}{Re} \left[\frac{\partial}{\partial \vec{r}} \cdot (\mu_1 \frac{\partial k}{\partial \vec{r}}) + G_k - \rho \varepsilon \right], \quad (5)$$

$$\rho \frac{\partial \varepsilon}{\partial t} + \rho \vec{V} \cdot \frac{\partial \varepsilon}{\partial \vec{r}} = \frac{1}{Re} \left[\frac{\partial}{\partial \vec{r}} \cdot (\mu_2 \frac{\partial \varepsilon}{\partial \vec{r}}) + C_1 \frac{G_k \varepsilon}{k} - C_2 \frac{\rho \varepsilon^2}{k} \right], \quad (6)$$

where $\hat{\tau}_{eff} = \mu_{eff} \hat{S} - \frac{1}{3}(\mu_{eff} \frac{\partial}{\partial \vec{r}} \cdot \vec{V} + Re\rho k) \hat{E}$; $\mu_{eff} = \mu + \mu_t$;

$D_{eff} = D_{1,2} + \mu_t Sc/Sc_t$; $\mu_1 = \mu + \mu_t/\sigma_k$; $\mu_2 = \mu + \mu_t/\sigma_\varepsilon$;

$\mu_t = Re^2 c_\mu \rho k^2/\varepsilon$; $G_k = \hat{\tau} \cdot \hat{S} + \frac{\mu_t}{Fr\, Sc_t} \frac{\partial C}{\partial \vec{r}} \cdot \frac{\vec{g}}{g}$.

The constants in the "k-ε" turbulence model, according to Spalding [11], are assumed to be: $C_1 = 1.44$, $C_2 = 1.92$, $c_\mu = 0.09$,

$\sigma_k=1$, $\sigma_\varepsilon=1.3$, $Sc_t=1$.

To take the laminar-turbulent transfer interaction into account which is significant in near-wall region, the wall function approach [12,13,14] is used:

$$\tau_w = \frac{\kappa\,\rho\,u_p\,\sqrt{k_p}\,\sqrt{c_\mu}}{\ln(E\,\sqrt{k_p}\,\sqrt{c_\mu}\,y_p\,/\,\nu)}\,, \qquad k_p = \frac{\tau_w}{\sqrt{c_\mu}}\,, \tag{7}$$

$$\varepsilon_p = \frac{c_\mu^{3/4}\,k_p^{3/2}}{\kappa\,y_p}\,, \qquad \left(\frac{\partial C}{\partial n}\right)_w = 0\,. \tag{8}$$

The relations (7)-(8) permit the imposition of boundary conditions for system (1)-(6) not directly at the solid wall but at the node "p", which is adjacent to the wall mesh point and must be located outside the viscous sublayer ($y_p^+=30$-100).

It should be noted that the non-evolutionary equation (2) is nothing else but a more general form of the incompressibility condition $\partial/\partial\vec{r}\cdot\vec{V}=0$, which is used in the Boussinesq approximation. It can be easily derived from the full continuity equation

$$\frac{\partial\rho}{\partial t} + \frac{\partial}{\partial\vec{r}}\cdot(\rho\vec{V}) = 0 \tag{9}$$

by expressing the density ρ as a function of the mass concentration C with the aid of the asymptotic form of the equation of state for a perfect gas mixture (4) and the contaminant mass conservation equation (3). Thus, from a mathematical point of view the system (1) - (4) does not principle differ from the Boussinesq approximation and, in particular, just like this model, does not posses any hyperbolic properties, which is the cause of the stiffness of the Navier - Stokes equations for compressible flows with low Mach numbers. Due to this advantage of the model one may use for its numerical solution almost the same methods as for solution of the incompressible flows or the Boussinesq equations, written in terms of $\vec{V}$-p variables (the use of the methods developed for the solving of the $\vec{\omega}$ - ψ form of the incompressible flow equations is impossible because the stream function ψ can not be introduced into the full continuity equation (9)).In particular,in the present work a modification of well known SMAC-method is used for this purpose. The velocity and pressure fields at the new time step are evaluated with a semi - implicit time advancement scheme for equations (1)-(2):

$$\rho^{\circ}\frac{\vec{V}^{n}-\vec{V}^{\circ}}{\tau}+\left[(\rho\vec{V}\cdot\frac{\delta}{\delta\vec{r}})\vec{V}\right]^{\circ}=-\frac{\delta p^{n}}{\delta\vec{r}}+\left[\frac{2}{Re}\frac{\delta}{\delta\vec{r}}\cdot(\hat{\tau}_{eff})+\frac{1}{\varepsilon_{m}Fr}(\rho-1)\frac{\vec{g}}{g}\right]^{\circ}, \quad (10)$$

$$\left(\frac{\delta\vec{V}}{\delta\vec{r}}\right)^{n}=S^{\circ},\ S^{\circ}=\frac{1}{Re\ Sc}\frac{\varepsilon_{m}}{(C\varepsilon_{m}+1)}\frac{\delta}{\delta\vec{r}}\cdot(D^{\circ}_{eff}\frac{\delta C^{\circ}}{\delta\vec{r}}) \quad . \quad (11)$$

For the numerical solution of (10)-(11) the following iterative procedure is used:

$$\vec{V}^{n}=\vec{V}^{\circ}-\tau(\vec{V}^{\circ}\cdot\frac{\delta}{\delta\vec{r}})\vec{V}^{\circ}-\frac{\tau}{\rho^{\circ}}\left\{\frac{\delta}{\delta\vec{r}}(p^{n})^{k-1}-\right.$$

$$\left.-\left[\frac{2}{Re}\frac{\delta}{\delta\vec{r}}\cdot(\hat{\tau}_{eff})+\frac{1}{\varepsilon_{m}Fr}(\rho-1)\frac{\vec{g}}{g}\right]^{\circ}\right\}, \quad (12)$$

$$(p^{n})^{k}=(p^{n})^{k-1}-\beta\left[\frac{\delta}{\delta\vec{r}}\cdot(\vec{V})^{n}-S^{\circ}\right], \quad (13)$$

where $\beta>0$ is an iterative parameter.

After the fields p^{n} and $\vec{V}^{n}$ have been calculated, the rest of the flow quantities are determined from equations (3)-(4) with the help of a finite-difference scheme by Patancar [15]. Space derivatives in (10)-(13) are approximated in a standard manner on a staggered mesh.

VERIFICATION OF THE COMPUTER CODE

To test the computer code VENTURE, developed for 2-D and 3-D simulations of VENtilation in TUrbulent REgimes on the basis of the model, described in previous section, some typical turbulent recirculating incompressible flows in rectangular rooms were calculated, which have been studied earlier experimentally or numerically. The room configurations and corresponding results of computations are presented in Fig.1. It can be seen that the agreement between numerical results of the present work and numerical and experimental data of other authors for all examined cases is fairly good.

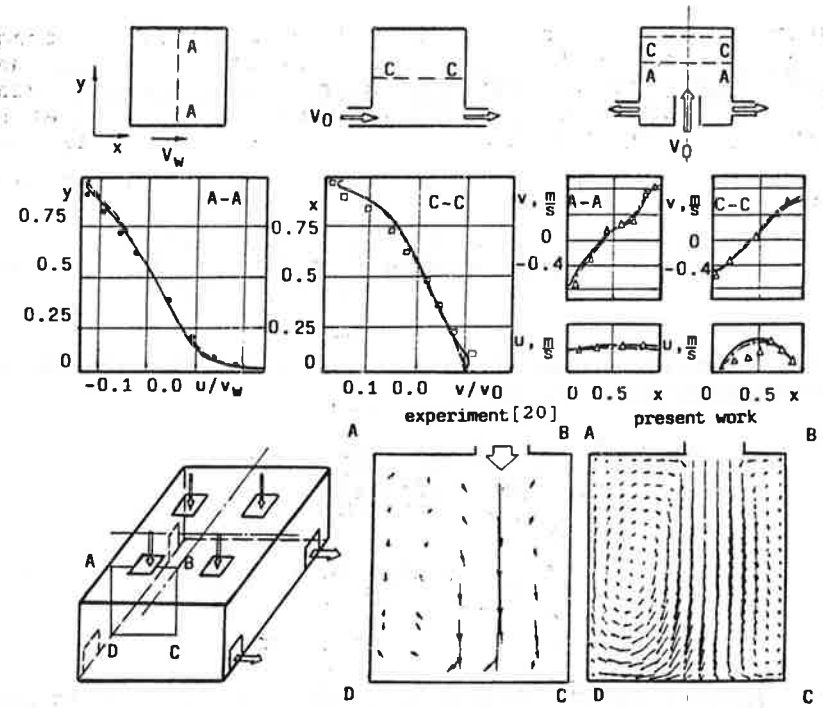

Fig.1. Comparison of computations of the present work (———) with numerical data by Ideriah [16] (----), by Boyle & Golay [17] (-·-·) and with experimental data by Grand [18] (····), by Girard and Curter [19](□□□□), by Boyle & Golay [17] (ΔΔΔΔ), and by Murakami, Kato, Suyama [20].

RESULTS AND DISCUSSION

The VENTURE code was used for the numerical investigation of unsteady turbulent mixed convection of binary gas mixtures in 2-D and 3-D rectangular rooms with inlet and outlet orifices. The flows of such a type are quite usual for accident situations, in connection with the contamination of a room by toxical or combustible gases.

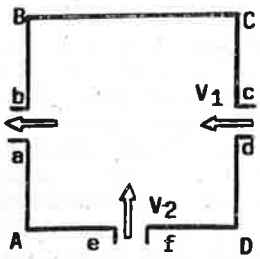

Fig.2. The scheme of 2-D room.

2-D Simulations. The geometry of the 2-D room and the location of the inflows and outflows are shown in Fig.2. It is assumed, that initially the inlet orifice "ef" is closed and there is a steady turbulent flow in the room, caused by its ventilation through inlet "cd" and outlet "ab". Then (at the moment t=0) the injection of a contaminant throught the orifice "ef" with velocity V_2 is started. A numerical

investigation of the transition from the initially steady flow in the room to the final one, corresponding to the new inflow boundary conditions, was carried out for a wide range of Reynolds and Froude numbers and the parameters $V_{2,1}=V_2/V_1$, $\varepsilon_m=m_2/m_1-1$ and $\ell=L_{CD}/L_{AD}$ (their values are summarized in Table 1 and results of the calculations are presented in Fig.3-5).

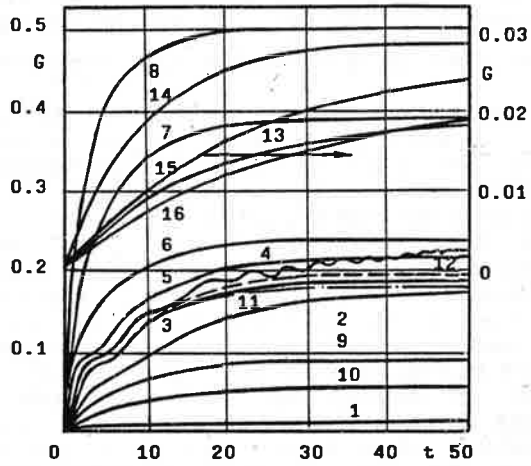

Fig.3. The time evolution of the integral mass fraction of contaminant (numbers at the curves correspond to the case numbers in Table 1).

Table 1.

N	Re	$V_{2,1}$	ε_m	Fr	ℓ	N	Re	$V_{2,1}$	ε_m	Fr	ℓ
1	10^4	0.01	1	1	1	9	10^4	0.5	3	1	1
2	10^4	0.3	1	1	1	10	10^4	0.5	6	1	1
3	10^4	0.5	1	1	1	11	10^4	0.8	1	0.5	1
4	10^4	0.8	1	1	1	12	10^5	0.5	1	1	1
5	10^4	1	1	1	1	13	10^5	0.01	1	1	1
6	10^4	2	1	1	1	14*	10^5	0.01	1	1	0.5
7	10^4	4	1	1	1	15*	10^5	0.01	1	1	1
8	10^4	6	1	1	1	16*	10^5	0.01	1	1	1.5

* - outlet orifice "ab" is on the wall "CD"

In all cases uniform profiles for all the flow quantities were imposed as boundary conditions at the inlet boundaries the values of k_{in} and ε_{in} at the inlet orifices being determined in correspondence with experimental data by Rheinlander [1]. The outflow boundary conditions were assumed as $\partial f/\partial n=0$ for all flow quantities except the

component of velocity vector, normal to the boundary, which was corrected to satisfy global conservation of gas volume (integral form of equation (2)).

The results of the calculations, presented in Fig.3-5, allow the analysis of the character and strength of the influence of the parameters, mentioned above, on the local flow characteristics and on the efficiency of ventilation, which may be judged from the time evolution of the integral mass fraction of foreign gas inside the room $G=\int_\Omega \rho C d\Omega / \int_\Omega \rho d\Omega$ (Fig.3). When analyzing these results, it should be mentioned first of all, that there exists a range of $V_{2,1}$ values for which the function G(t) is non-monotonic (see curves 2-5 in Fig.3). Analogous phenomenon was found earlier by Niculin & Strelets [9,10] for laminar regimes of the flow under consideration. However in the case of laminar flows undamped auto-oscillations take place in such situation, whereas for turbulent regimes these oscillations, arising at initial stage of the process, appear to be damped asymptotically when $t \to \infty$ (see Fig.3). Such qualitative difference in the behavior of laminar and turbulent flows is caused by the intensive turbulent diffusion of the light contaminating that prevents the periodical formation of a local zone with low density in the bottom part of the room, resulting in auto - oscillations in laminar flows [9].

Fig.4 illustrates the influence of the value of $V_{2,1}$ on the averaged mass fraction G of the contaminant and its maximum value at the top wall of the room $(C_w)_{max}$ at the steady stage of the process (t=50) for $Re = 10^4$, Fr = 1, ε = 1.

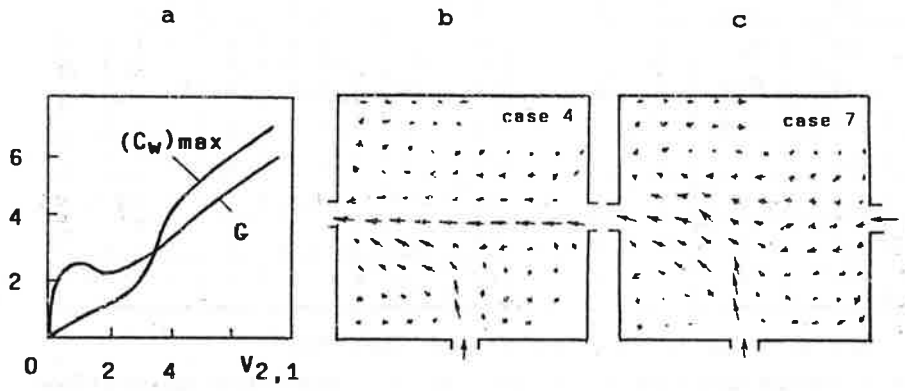

Fig.4.The influence of the value $V_{2,1}$ on the averaged mass fraction of contaminant and its maximum value at the top wall (a)and velocity field for $V_{2,1}$=0.8 (b) and $V_{2,1}$=4 (c) for flow conditions according cases 4, 7 in Table 1.

The change in the character of the curves in the neighbourhood of $V_{2,1} = 2$, clearly seen in Fig.4, is explained by the change in the flow structure near this value of the parameter. When $V_{2,1} < 2$ the jet of light gas, entering into the room through the orifice "ef", can not overcome shielding action of ventilating jet (see Fig.4,case4). That results in the accumulation of the light gas mainly in the bottom part of the room. When $V_{2,1} > 2$ the contaminating jet goes through the ventilating jet (see Fig.4, case 7) and the rate of growth of both $(C_w)_{max}$ and G increases sharply as $V_{2,1}$ increases.

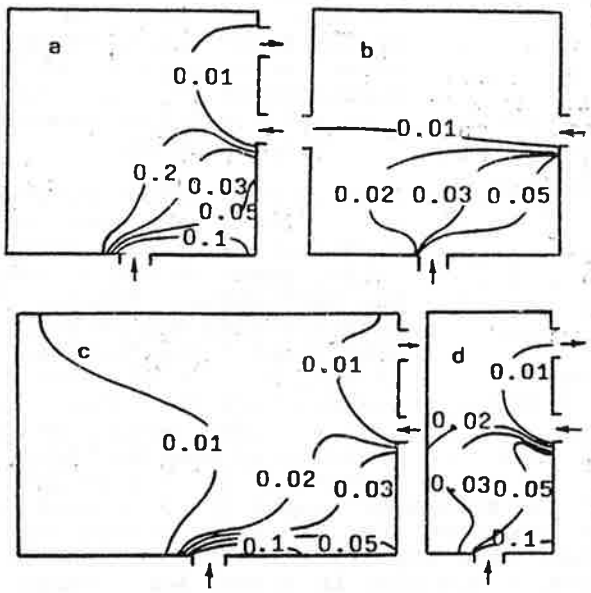

Fig.5. The field of mass fraction of the contaminating gas for the room with different geometries (at t=50, a-case 15, b-13, c-16, d-14 in Table 1).

One of the most important problems in the design of ventilation systems is the problem of choice of the positions of the inlets and outlets providing the desired properties of the system. Fig.5 shows that the integral models of ventilation processes, being of common use in design practice, can scarcely be used for solving this problem because they do not take into account such important effects as the significant changing of the flow structure and contaminant spatial distribution when varying geometry of the room and positions of the inlets and outlets.

3-D Simulations. As an example of the application of the VENTURE code to the 3-D simulation we present some results for the ventilation of the room which was studied by Murakami, Kato, Suyama [20] (see the bottom part of Fig.1)

and is referred to as "empty" room bellow. The other room which was studied (the "blocked up" room) differs from the first one by additional four bodies located on the floor directly under the inlet orifices and shaped as rectangular parallelepipeds with the dimension of plane 0.4 × 0.45 and height 0.5 (the scale of the length is the total room's height). As in the 2-D case, it is assumed that initially there is a steady flow of ventilation air in the room. For the "empty" room the velocity field of such flow at the plane ABCD is presented in Fig.1 and for the "blocked up" room - in Fig.6. At the moment t=0, foreign gas (CH_4, Cl_2 or H_2) starts to penetrate into the room through the hole in the center of the floor with a velocity V_2 and after some period of time Δt supplying of this gas is broken up (in the simulation discussed bellow V_2= 3m/s and Δt=3s).

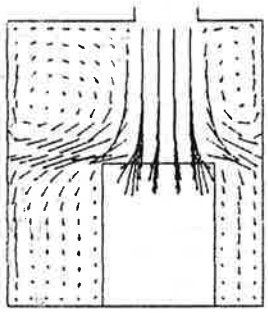

Fig.6. Steady ventilation velocity field for the "blocked up" room

Fig.7,8 illustrate the evolution of the flow structure and spatial distribution of different contaminating gases at the initial stage of the ventilation process (while the contaminating gas is supplied) for both "empty" and "blocked up" rooms. It can be clearly seen from these figures that the influence of the kind of the contaminating gas is drastically depends upon the room geometry. In particular, for the "empty" room the molecular weight of the contaminating gas plays crucial role and significantly affects the character of the process (see Fig.7). For the "blocked up" room the role of buoyancy effects is great deal weaker: both the velocity fields and the contours of different contaminating gases volume fraction differ from each other relatively slightly (see Fig.8). It is caused by the constraining action of the embedded bodies, which prevent the process of spreading of the heavy contaminating gas (for instance Cl_2) along the floor of the room due to the buoyancy effects.

The second stage of the ventilation process (after the breaking up of supplying of the contaminating gas) is illustrated by Fig.9. Again both the structure of the ventilation flow and contaminating gas spatial distribution inside the room are quite different for the cases of "empty" and "blocked up" room, the ventilation efficiency being significantly higher for the last case. More clearly this fact is seen from the Fig.10, where the averaged volume fractions of H_2 and Cl_2 are plotted as the functions of the time. Even though the relative content of the contaminating gas in the "blocked up" room is higher than that in the "empty" room at the moment of breaking up the supplying of the contaminant the rate of its removing from the "blocked up" room is much faster. This results in the

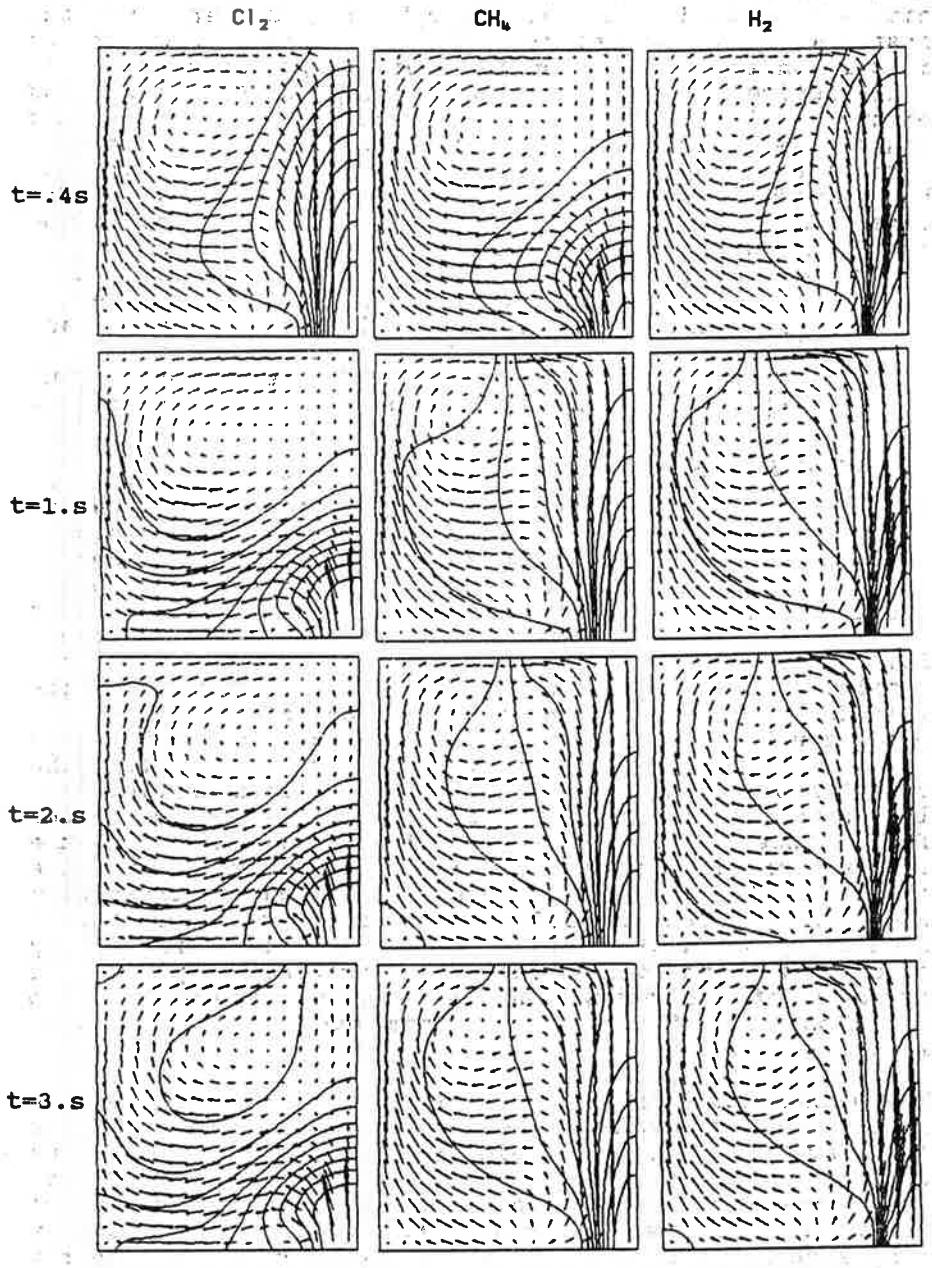

Fig.7. The time evolution of velocity field and contours of volume fraction of the contaminating gas X at the vertical symmetry plane parallel to the plane ABCD for the "empty" room: $X_{max}=0.9$, $X_{min}=0.1$, $\Delta X=0.1$.

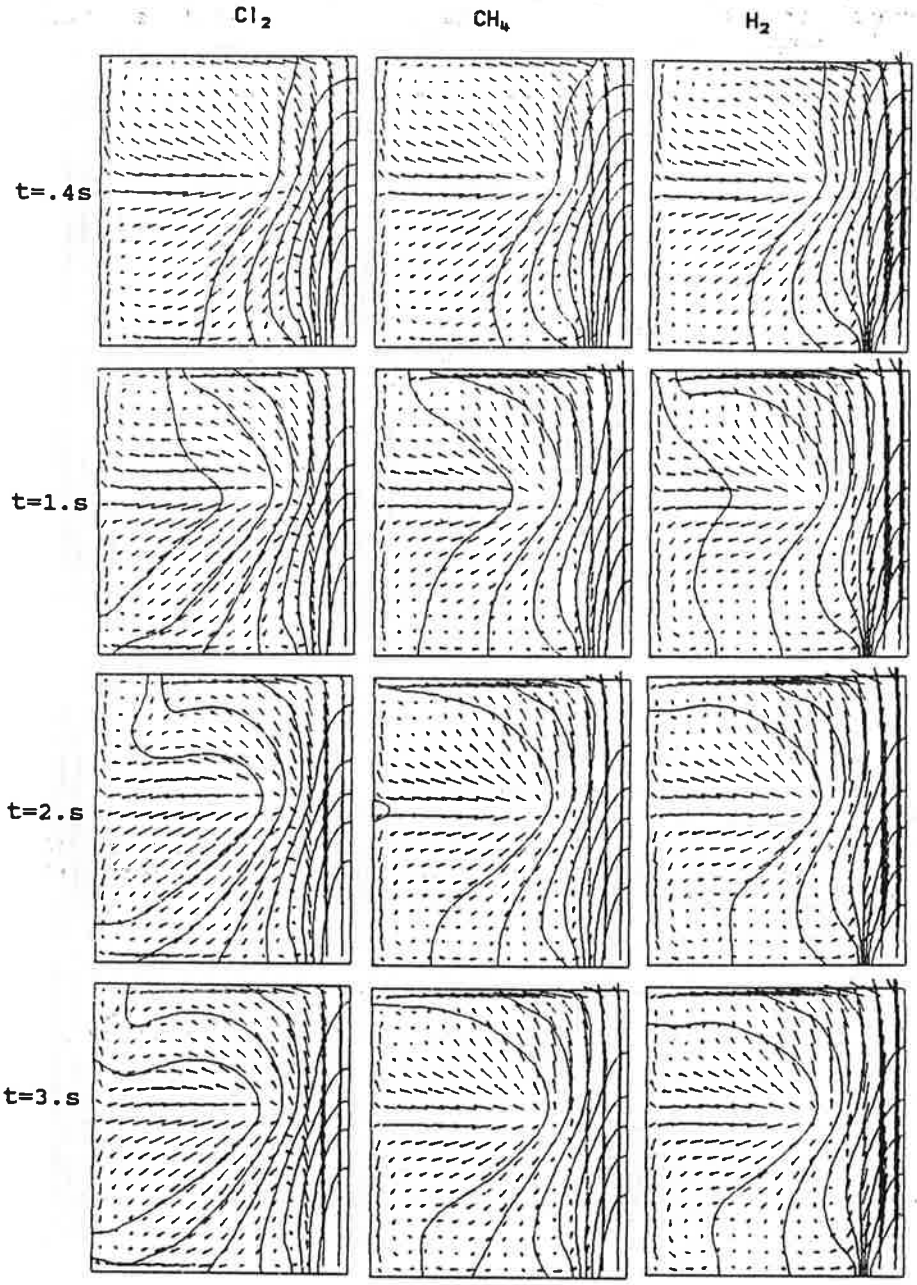

Fig.8. The time evolution of velocity field and contours of volume fraction of the contaminating gas X at the vertical symmetry plane parallel to the plane ABCD for the "blocked up" room: $X_{max}=0.9$, $X_{min}=0.1$, $\Delta X=0.1$.

fact that the content of the contaminant at the end of the process for the "blocked up" room is great deal lower than for the "empty" one.

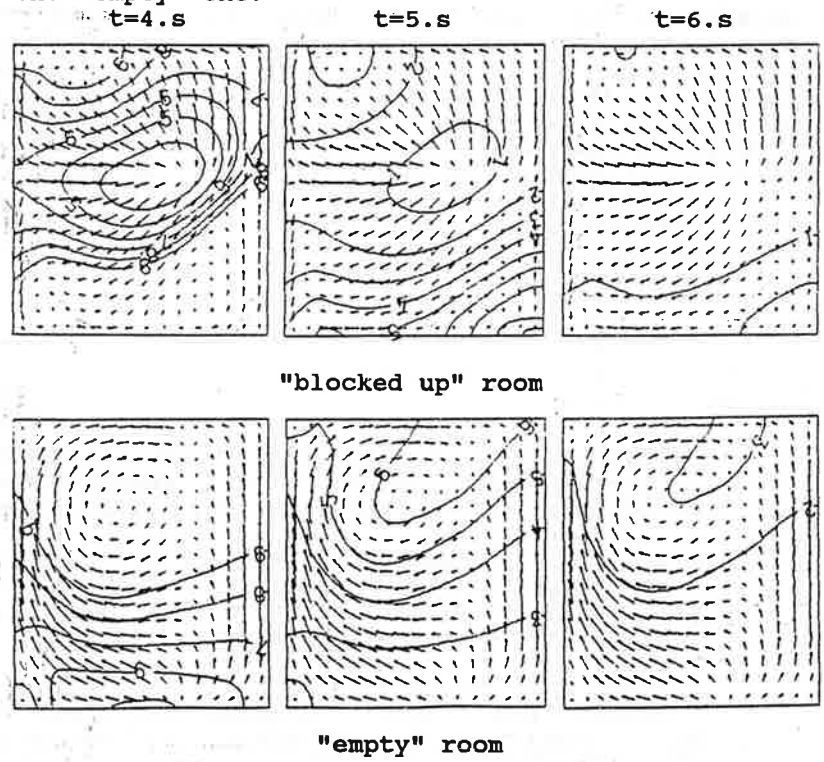

Fig.9. The time evolution of velocity field and contours of volume fraction of the contaminant X at the vertical symmetry plane parallel to the plane ABCD: 1-X= 0.01,..., 9-X= 0.09.

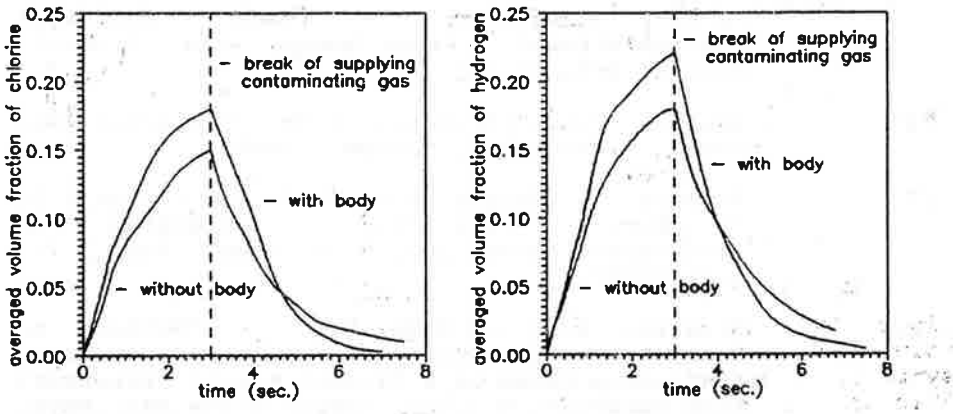

Fig.10. The time evolution of averaged volume fraction of the contaminant.

CONCLUSION

A new asymptotic (low Mach number) model for the turbulent ventilation flows simulation is proposed. An important advantage of the model over traditional Boussinesq approximation is its applicability to the description of flows with large density gradients, caused by the great difference between the molecular weights of the ventilating and contaminating gases. The capabilities of the model and of the developed computer code VENTURE have been demonstrated by examples of its application to the numerical simulation of unsteady ventilation flows in both 2-D and 3-D geometries.

LITERATURE

[1] Rheinlander, J. " Numerische Berechnung von vorwegend durch die Schwerkraft angetricbenen Raumstromungen". Fortschr-Ber.VDI-z,174,(1981).

[2] Nielsen,P.V. "Numerical Prediction of Air Distribution in Rooms - Status and Potentials". In Building Systems: Room Air Contaminant Distribution, ASHRAE,(1989)

[3] Nielsen,P.V. "Airflow Simulation Techniques - Progress and Trends". Progress and Trends in Air Infiltration and Ventilation Research, 10th AIVC Conference, Finland, (1989).

[4] Oran,E.S. and Boris, J.P.,"Numerical Simulation of Reactive Flow". Elsevier Publ., New York - Amsterdam - London,(1987).

[5] McDonald, H."Combustion Modelling in Two and Three Dimensions - Some Numerical Considerations". Progr.Energy and Combust. Sci.,5, No2, 97-122 (1979).

[6] Lapin,Yu.V.and Strelets, M.Kh. "Internal Gas Flow". Nauka Publ., Moscow, (1989).

[7] Patnaik,G., Guirguis,R.H.,Boris,J.P., Oran,E.S. "A Barely Implicit Correction for Flux-Corrected Transport". J. Compt. Phys., 71, 1-20 (1987).

[8] Strelets, M.Kh.and Shur, M.L. "Methods of Scaling the Compressibility in Calculating Stationary Flows of a Viscous Gas at Arbitrary Mach Numbers". U.S.S.R. Comput.Maths.Math.Phys. 28,165-173 (1988).

[9] Niculin, D.A. and Strelets, M.Kh. "On the Possibility of Self-Oscillatory Solutions of Nonstationary Problems of Mixed Convection in Gas Mixtures".Sov.Phys.Dokl.26,844-845 (1982)

[10] Niculin,D.A. and Strelets M.Kh. "Calculation of Nonstationary Mixed Convection of Binary Gas Mixtures in the Presence of Lardge Density Variations"J.Appl.Mech.Tech.Phys.25,50-56(1984)

[11] Spalding D.B. "Turbulence Models". Imperial College Mechanical Engineering Dept. Report HTS/76/17 (1976).

[12] Rodi, W. "Turbulence Models and their Application in Hydraulics - A State of the Art Review". University of Karlsruhe SFB 80/T/127 (1978).

[13] Ng, K.H.and Spalding, D.B."Turbulence Model for Boundary Layers near Walls". Physics Fluids, No 15, 20-30 (1972)

[14] Launder, B.E.and Spalding, D.B. "Mathematical Models of Turbulence". Academic Press, London, (1972).

[15] Patankar,S. "Numerical Heat Transfer and Fluid Flow". Hemisphere Publ. New York, (1980).

[16] Ideriah, F.J.K. "On Turbulent Forced Convection in a Square Cavity". Proc. 1 - st Int. Conf., Numer. Meth. in Laminar and Turbulent Flow.- London: 257-269 (1979).

[17] Boyle, D.R.and Golay, M.W. " Measurement of Recirculating, Two - Dimensional, Turbulent Flow and Comparison to Turbulence Model Predictions. 1.Steady State Case". Trans. ASME.J.Fluids Eng. 105, No 4,439-446 (1983).

[18] Grand, D. "Contribution a l'etude des courants de recirculation". Ph. D. Thesis, L'Universite Scientifique et Medicale et inst. Nat. Pol., Grenoble (1975).

[19] Girard, J.Ph.and Curter, R. "Etude des courants de recirculation dans une cavite". Report CEA GR - 751-354, Inst. de Mecanique Domain Universitaire.Grenoble (1975).

[20] Murakami, S.,Kato, S., Suyama, Y. "Three - Dimensional Numerical Simulation of Turbulent Airflow in a Ventilated Room by Mean of a Two-Equation Model". ASHRAE Transactions, 93 (Pt2),621-641 (1987).